Hindawi
Advances in Materials Science and Engineering
Volume 2020, Article ID 6089482, 9 pages
https://doi.org/10.1155/2020/6089482

Research Article

Effects of Nano-SiO_2 and SAP on Hydration Process of Early-Age Cement Paste Using LF-NMR

Haitao Zhao,[1] **Yi Wan**,[2,3] **Jun Xie**,[4] **Kaidi Jiang**,[3] **Donghui Huang**,[5] **Xiaodong Chen**,[3,6] **Shihai Li**,[3] **Ruiming Jia**,[3,7] **and Gaoyang Sun**[3,8]

[1]*College of Materials Science and Engineering, Southeast University, Nanjing 211189, China*
[2]*Anhui Transport Consulting & Design Institute Co., Ltd, Hefei 230088, China*
[3]*College of Civil and Transportation Engineering, Hohai University, Nanjing 210098, China*
[4]*Nanjing Power Supply Company, State Grid, Nanjing 210019, China*
[5]*School of Architectural Engineering, Jinling Institute of Technology, Nanjing 211169, Jiangsu, China*
[6]*China Communications Construction Urban Investment Holding Co., Ltd., Guangzhou 510623, China*
[7]*Tong Yuan Design Group Co., Ltd, Jinan 250101, China*
[8]*Jiangsu Testing Center for Quality of Construction Engineering Co., Ltd., Nanjing 210028, China*

Correspondence should be addressed to Haitao Zhao; hhuzhaoht@163.com

Received 12 July 2019; Accepted 21 February 2020; Published 23 March 2020

Academic Editor: Candido Fabrizio Pirri

The effects of nano-SiO_2 and superabsorbent polymer on the hydration process of early-age cement paste are investigated through the physically bound water evolution test by means of the low-field nuclear magnetic resonance technology. The test results show that the hydration process can be characterized by four-stage patterns based on the zero points of the second-order differential hydration curve, i.e., the initial, accelerated, decelerated, and steady periods. The beginning time of each stage is postponed and the hydration duration is prolonged with an increasing water to cement ratio. The beginning time of each stage and the hydration duration are shortened with an increasing content of nano-SiO_2. And the beginning time of each stage and the hydration duration are prolonged with an increasing content of superabsorbent polymer. Based on the test data and the Avrami–Erofeev model, a modified hydration model taking the influence of nano-SiO_2 and SAP into account is proposed, and the predicted results are consistent with the test results.

1. Introduction

Nanomaterials had been increasingly used in the construction and building materials with the rapid development of nanomaterials. Nanomaterials are defined as the materials with particle sizes which are less than 100 nm and have many excellent properties which differ from those of traditional materials [1, 2]. Previous studies have shown that the addition of nanomaterials can effectively enhance the physical and mechanical properties of cement-based materials (CBMs) [3, 4]. At present, the addition of nano-SiO_2 (NS) in CBM is one of the research priorities. In addition, the internal humidity field is closely related to the early-age crack of CBM [5]. The internal curing (IC) of CBM can improve the internal humidity field in CBM [6]. Therefore, the IC method can mitigate the autogenous shrinkage (AS) and the early-age crack risk of CBM. Meanwhile, superabsorbent polymer (SAP) has a relatively slight influence on the strength of concrete compared with other IC materials. As a result, SAP is an ideal internal curing material and is a hot spot in the field of building materials research. So far, researchers have focused on the study of the traditional physical and mechanical properties of CBM with NS [7]. Qing et al. [8–10] found that NS had higher pozzolanic activity than ordinary silica fume. When the content of NS was about 3% replacement of cement, the strength of cement paste could be improved by nearly 50%. Zhang et al. [11] investigated the strength of fly ash concrete which was doped

with NS and found that when the NS content was 2% replacement of cement, the strength of cement paste at 7 days was improved by nearly one-third. The results of Said et al. [12] also showed that when the NS content was less than 6%, the strength of concrete will be improved. Singh et al. [13] found that NS could accelerate the cement hydration reaction, and with the NS content increasing, the hydration rate also increased. Sneff et al. [14] investigated the effects of NS on the hydration heat of cement paste and the results suggested that the addition of NS made the peak of cement hydration heat increased, the arrival time of hydration heat peak shortened, and the reaction rate accelerated obviously. However, although NS could promote the CBM hydration, it would consume more water at the same time, which could increase the early-age AS of CBM. Guo et al. [15] have shown that the AS of concrete with NS was higher than that of concrete without NS. It was considered that the early high activity of NS made the hydration speed faster and the relative humidity was reduced. Meanwhile, SAP can be added to the cement-based materials to introduce extra water and compensate the water consumed by hydration. Therefore, the addition of SAP to the NS CBM can ensure the hydration of the cement paste more completely and decrease self-shrinkage. Over the years, some researches have been conducted on the hydration process of CBM with the addition of SAP. Esteves [16] researched the hydration degree of cement pastes and mortars by the means of the differential thermogravimetric analysis and found that the hydration of the cement paste was accelerated by the SAP addition. The research of Justs et al. [17] also indicated that SAP could promote the hydration of cementitious materials at the ages of 7 and 28 days. However, the research on the combined influences of NS and SAP on the hydration of CBM was lacking.

How to monitor the hydration process is important in contemporary cement hydration research. The traditional methods are a determination of hydration heat, resistivity method, electron microscopy method, and so on. The determination of hydration heat researches the hydration of cement by testing hydration heat, but it is not suitable to the composite pastes and cannot well characterize the later hydration process due to its low hydration heat [18]. Xiao et al. [19] developed a contactless resistivity meter using the principle of the transformer, which eliminated the electrode and solved the contact problem of the traditional resistivity method, though the alternating current measurement is relatively complicated and the selection of frequency has an influence on resistivity. Transmission electron microscopy (TEM) and scanning electron microscopy (SEM) are widely employed to monitor concrete hydration, but the sample preparation of the two methods is complex, and the microstructure of the sample is likely to be damaged in the sample preparation process. Nowadays, low-field nuclear magnetic resonance (LF-NMR) is applied to monitor the physically bound water content in the cement paste on the ground of proton relaxation characteristics of water molecules and to characterize the hydration of cementitious materials [20, 21]. Compared with the traditional methods, LF-NMR has the advantages of noninvasive, nondestructive, and continuous measurement; therefore, it can realize the nondestructive continuous monitoring of the cement hydration process. Apih et al. [22] reported that the longitudinal relaxation time (T_1) of the cement paste declined along with the cement paste hydration, which could be used to indicate the stages of the hydration of cement. She et al. [23] characterized the hydration process of the cement paste and described and analysed the hydration process of cement paste in detail by testing the T_1 of cement paste by employing LF-NMR. The T_1 test needs longer time than T_2 (i.e., transverse relaxation time) and T_1 is more affected by the test parameters. An-ming et al. [24] also found that the development of T_2 could well depict the kinetics of hydration, and the initial period, the accelerated period, and the steady period were categorized according to the difference in changing rate. Zhao et al. [25] investigated the influence of nano-$CaCO_3$ and superabsorbent polymer on the hydration process of early-age cement paste and found that the T_2 of LF-NMR could well characterize the hydration process of early-age cement paste.

In the present study, the influences of water-to-cement ratio (w/c), NS, and SAP on the hydration process of the cement paste were studied by employing LF-NMR. Furthermore, a prediction model of hydration taking the influences of NS and SAP into account was proposed.

2. Materials and Methods

2.1. Materials. P II52.5 Portland cement with a specific surface area of 350 m^2/kg and the density of 3180 kg/m^3 was employed. Table 1 shows the chemical compositions of the cement. The purity of the NS is 99% by weight and its grain size is less than 20 nm. Besides, an organic-inorganic polymer material is used as the SAP, and the water absorption capacity of which is 20 g water/g SAP.

The w/c, dosage of NS, and SAP were considered as the influencing factors of the hydration. The category of samples is shown in Table 2. 0.30NS1.5P0.15 represents the sample with the 0.30 of w/c, 1.5% for NS content, and 0.15% for SAP content. The lasting time of each sample test is 96 hours.

2.2. Sample Preparation. All the test samples were prepared by applying the mixing procedure according to the method mentioned in ASTM C-305 [26].

2.3. Testing Methods. The hydration tests of all the samples were processed on a PQ001 LF-NMR with 0.42 T of magnetic field and 18 MHz of proton frequency field. The samples were placed in a room with a temperature of 20 ± 1°C.

Before the test, the width of the $\pi/2$ pulse (P1) and the offset of RF signal frequency (O1) were gained by calibrating the free induction decay (FID) sequence of the oil sample. Then, the transverse relaxation time T_2 of pastes was measured by applying the Can-Purcell-Meiboom-Gill (CPMG) sequence ($\pi/2$–[τ–π–τ]n-TR), where $\pi/2$ and π were pulses which could make the magnetization vector rotate around the axis where pulses were applied; n was the number of sampling data and TR was the interval between

Table 1: Chemical compositions of cement.

Component	SiO_2	Al_2O_3	Fe_2O_3	CaO	MgO	Na_2O	K_2O	SO_3	TiO_2	LOI
Percentage of mass	19.53	4.31	2.89	63.84	1.25	0.13	0.64	3.25	0.26	3.00

Table 2: Category of cement paste.

Sample	w/c	NS content (%)	SAP content (%)	Water reducing agent (%)	Influence factor
0.30NS0.0	0.30	0	0	0.2	w/c
0.35NS0.0	0.35	0	0	0.1	
0.40NS0.0	0.40	0	0	0.0	
0.30NS1.0	0.30	1.0	0	0.2	NS content
0.30NS1.5	0.30	1.5	0	0.2	
0.30NS2.0	0.30	2.0	0	0.2	
0.30NS3.0	0.30	3.0	0	0.2	
0.30NS1.5P0.15	0.30	1.5	0.15	0.2	SAP content
0.30NS1.5P0.30	0.30	1.5	0.30	0.2	

two adjacent tests. The set of the parameters on LF-NMR are shown in Table 3.

A(t), the wave crest amplitude of the T_2 signal, is used to characterize the hydration process and is shown in Figure 1. Then, the curve of A(t) in unit mass cement paste is obtained (see Figure 2). Figure 2 shows that the hydration process could be categorized into four stages: the initial, accelerated, decelerated, and steady periods according to the zero points (b_1, b_2, and b_3) of the second-order differential curve (see Figure 3) [25].

3. Results and Discussions

3.1. Effects of w/c on the Cement Paste Hydration. Figure 4 shows the influence of w/c on the T_2 signal amplitude (TSA) in unit mass cement paste. It can be seen from Figure 4 that the increase of the w/c leads to the increase of TSA during the hydration. The larger the w/c, the much the physically bound water in the unit mass cement paste, and then the greater the signal quantity of the physically bound water. The test data is subjected to the differential treatment according to the method introduced above and then the time cut-off point of the four periods is obtained and the results are shown in Figure 4 and Table 4.

The hydration of the samples 0.30NS0.0, 0.35NS0.0, and 0.40NS0.0 is mild in the initial period (0.0–t_1), and the decline of TSA in unit mass is not obvious. The reason is that the C_3S takes part in the reaction rapidly in this period, and calcium silicate hydrate (C-S-H) covers the surface of the cement particles. As a result, it hampers the dissolution of the cement clinker mineral phase. At the same time, it can decrease the diffusion rate of ions (e.g., SO_4^{2-} and OH^-) which pass through the coating of ettringite taking part in the reaction. As a result, it impedes the further rapid progress of hydration. As can be seen from Figure 4 and Table 4, the duration of the initial period of the samples 0.30NS0.0, 0.35NS0.0, and 0.40NS0.0 is 1.52, 1.72, and 1.97 h, respectively. Therefore, the initial period increases with w/c.

The accelerated period (t_1-t_2) begins at the end of the initial period. At this period, the slope of the curve becomes larger; that is, the rate of physical water signal descending in the paste is accelerated, which indicates that the hydration is accelerated. As a reason, with the partial dissolution of C_3S, the concentration of $Ca(OH)_2$ in the solution continues to increase until it reaches supersaturation, and then $Ca(OH)_2$ rapidly nucleates and grows, making the calcium ion concentration of liquid phase decrease significantly and promote the hydration of C_3S as well as the precipitation of substantial C-S-H crystal nucleus. Meanwhile, as C_3S continues to be hydrated, the coating on the surface of cement particles continues to be thickened and begins to crack partly under the crystallization pressure. Consequently, a new anhydrous surface is exposed and the cement hydration is accelerated. As shown in Table 4, compared with the sample 0.30NS0.0, t_1 of the samples 0.35NS0.0 and 0.40NS0.0 delay for 0.20 and 0.45 h, respectively. Therefore, the increase of w/c delays the arrival of the accelerated period of cement paste. In addition, the duration of the accelerated period of 0.30NS0.0, 0.35NS0.0, and 0.40NS0.0 is 3.40, 3.60, and 3.70 h, respectively; that is, with the increase of w/c, the duration of the accelerated period is longer. During the decelerated period (t_2-t_3), the hydration rate of paste gradually slows down. The reasons are as follows. The hydration rate in this period is mainly controlled by both mineral hydration and diffusion reaction. On the one hand, as the hydration reaction goes on and hydration products continue to be generated and overlapped with one another, the spatial network structure is finally formed. The surface of cement particles is gradually covered by the hydration products, which make cement particles dissolved difficultly. On the other hand, with the consumption of physically bound water, the pastes begin to harden after losing its plasticity. It can be seen from Table 4 that, compared with the sample 0.30NS0.0, t_2 of the samples 0.35NS0.0 and 0.40NS0.0 delay for 0.40 and 0.75 h, respectively. Thereby, the increase of w/c delays the arrival time of the decelerated period of cement paste. And the duration of the decelerated period of 0.30NS0.0, 0.35NS0.0, and 0.40NS0.0 is 28.08, 29.68, and 31.33 h, respectively. In short, with the increase of w/c, the duration of the decelerated period is longer.

Table 3: Parameter settings for LF-NMR.

Sequence	TD	SW	RFD	RG1	DRG1	PRG	TW	NS	NECH	TE	DL1
FID	1024	100	0.02	20	3	2	2000	4	—	—	—
CPMG	Automatic settings	250	0.005	10	3	2	200	16	500	0.11	500

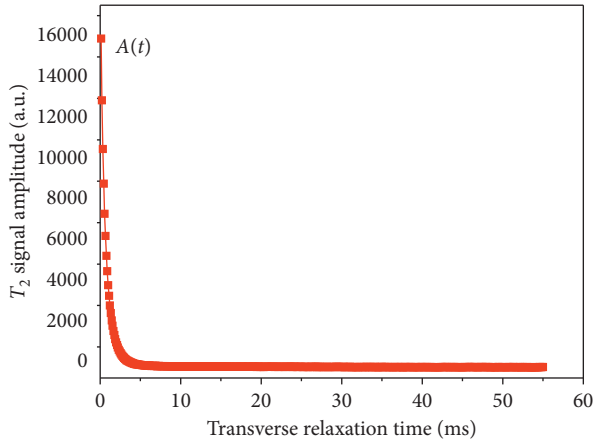

Figure 1: First wave crest amplitude of T_2 signal.

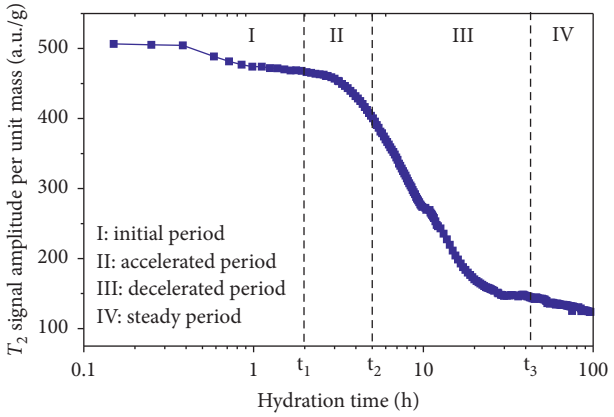

Figure 2: The first peak amplitude A(t) in unit mass changes with time.

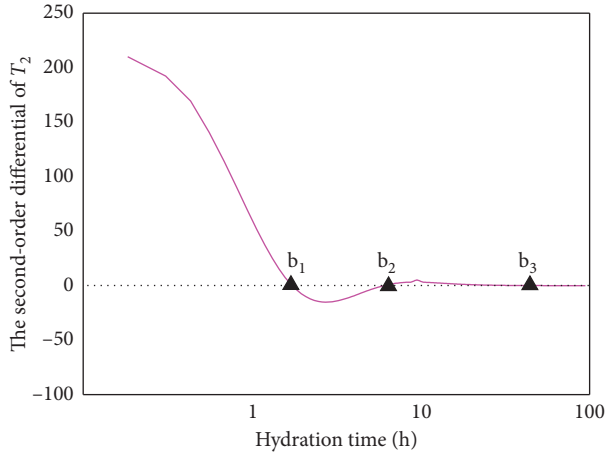

Figure 3: Second-order differential of A(t).

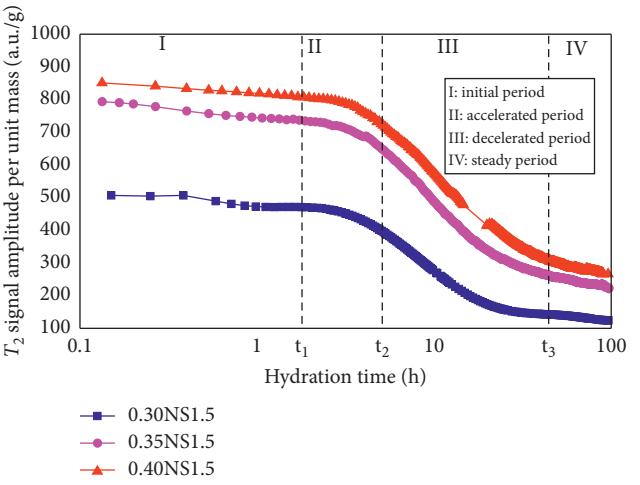

Figure 4: Effects of different w/c on the hydration process.

Table 4: The hydration period separation time of different w/c pastes (h).

Sample	t_1	t_2	t_3
0.30NS0.0	1.52	4.92	33.0
0.35NS0.0	1.72	5.32	35.0
0.40NS0.0	1.97	5.67	37.0

As can be observed from Figure 4, the hydration rate is low and stable after hydration for 30 h; then, it achieves a steady period ($>t_3$). At this stage, the surface of the cement mineral is almost covered and the cement hydration reaction rate is mainly controlled by the diffusion reaction [27]. The TSA of 0.30NS0.0, 0.35NS0.0, and 0.40NS0.0 at 96 h is 124.7, 223.9, and 366.3 a.u./g, respectively. Thus, the physical bound water signal in the cement paste significantly increases with w/c. Moreover, compared with the sample 0.30NS0.0, t_3 of 0.35NS0.0 and 0.40NS0.0 are advanced 2.0 and 4.0 h, respectively. So, the increase of w/c delays the arrival time of the steady period of cement paste.

3.2. Effects of NS on the Cement Paste Hydration. The curves of TSA in unit mass of cement paste with 0%, 1.0%, 1.5%, 2.0%, and 3.0% content of NS are shown in Figure 5. It can be observed from Figure 5 that the NS dosage had an obvious influence on each stage of hydration. The hydration process can be divided into four periods as mentioned above, and the duration of each period is listed in Table 5. The more the NS dosage, the stronger the TSA in unit mass cement paste. As binder materials hydrate continuously, the TSA in all samples of cement paste declines with different decreasing rates.

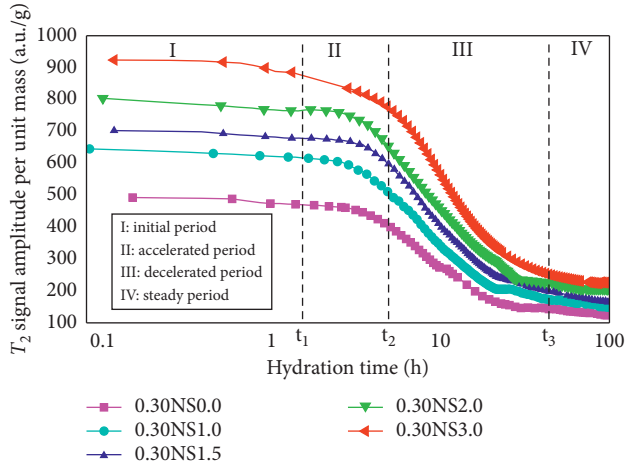

Figure 5: Effects of different dosages of NS on the hydration process.

Table 5: The hydration period separation time of different NS content cement pastes (h).

Sample	t_1	t_2	t_3
0.30NS0.0	1.52	4.92	43.85
0.30NS1.0	1.47	4.85	42.22
0.30NS1.5	1.45	4.78	41.42
0.30NS2.0	1.27	4.36	40.60
0.30NS3.0	1.18	4.06	39.75

The TSA of 0.30NS0.0, 0.30NS1.0, 0.30NS1.5, 0.30NS2.0, and 0.30NS3.0 decreases by 22.0, 22.1, 23.0, 28.0, and 28.8 a.u./g, respectively, at the end of the initial period (0.0–t_1). Furthermore, it shows that, with the addition of NS, the decrease rate of TSA is increasing, and it becomes more obvious with the increase of NS content. Besides, the duration of 0.30NS0.0, 0.30NS1.0, 0.30NS1.5, 0.30NS2.0, and 0.30NS3.0 in the initial period is 1.52, 1.47, 1.45, 1.27, and 1.18 h, respectively, pointing out that with NS content increasing, the initial period lasts shorter. The reasons are as follows. The hydration equation of C_3S can be written as $2C_3S + 6H \longrightarrow C_3S_2H_3 + 3CH$ [28]. On the one hand, due to the strong early activity of NS, it can react to hydration products $Ca(OH)_2$ [29]. On the other hand, due to the adsorption effect of nanoparticles, the concentration of Ca^{2+} decreases. These two reasons can jointly promote the hydration reaction to the right; thus, it can accelerate the dissolution rate of C_3S and promote the cement hydration.

With more NS addition, the decrease of TSA is enlarged in the accelerated period (t_1-t_2). During this period, the TSA of 0.30NS0.0, 0.30NS1.0, 0.30NS1.5, 0.30NS2.0, and 0.30NS3.0 decreases by 66.0, 105.0, 106.0, 111.0, and 137.0 a.u./g, respectively. Compared with 0.30NS0.0, the decrease signal amplitude of 0.30NS1.0, 0.30NS1.5, 0.30NS2.0, and 0.30NS3.0 increases by 59.0%, 61.0%, 68.0%, and 74.0%, respectively. The results show that the addition of NS can significantly increase the decrease of TSA, and the relationship between the decreased amplitude and the NS content is positive. Besides, the duration of 0.30NS0.0, 0.30NS1.0, 0.30NS1.5, 0.30NS2.0, and 0.30NS3.0 in accelerated period is 3.40, 3.38, 3.33, 3.09, and 2.88 h, which are shortened with the increase of NS dosage, showing the same effect of accelerating the hydration process of cement pastes as that during the initial period, as reported in Land and Stephan [30]. One reason for the influence of NS in this period is that the NS particles have a large specific surface area and C-S-H seeds are formed on the NS particles surface to accelerate the C_3S hydration. And this acceleration is more significant when the NS content is larger due to more C-S-H seeds forming.

Compared to 0.30NS0.0, the decline rate of TSA per unit mass of 0.30NS1.0, 0.30NS1.5, 0.30NS2.0, and 0.30NS3.0 is larger in the decelerated period (t_2–t_3), which suggests that NS enables the hydration rate of cement pastes to speed up. During this period, the average descending rates of physically bound water signals are 6.9, 9.1, 10.9, 11.9, and 3.62 a.u./g/h, respectively. Besides, TSA of 0.30NS0.0, 0.30NS1.0, 0.30NS1.5, 0.30NS2.0, and 0.30NS3.0 decreases by 268.0, 339.0, 399.0, 433.0, and 508.0 a.u./g, respectively. It shows that TSA decreases markedly during the decelerated period with the addition of NS. And the decelerated period of 0.30NS0.0, 0.30NS1.0, 0.30NS1.5, 0.30NS2.0, and 0.30NS3.0 lasts for 38.93, 37.37, 36.64, 36.24, and 35.69 h, respectively. Obviously, with the increase of NS content, the duration of the decelerated period shortens. It is because that the hydration of C_3S and C_2S is temporarily delayed returning to normal level due to the complete destruction of the protective layer, and cement paste with large NS dosage makes the dissolution of cement minerals slow because the high surface area of NS has a high ability to absorb ions.

At 96 h of hydration, TSA of 0.30NS0.0, 0.30NS1.0, 0.30NS1.5, 0.30NS2.0, and 0.30NS3.0 lessens to 124.0, 150.0, 165.0, 206.0, and 225.0 a.u./g, respectively. These quantities are just 25.3%, 24.0%, 23.9%, 26.4%, and 24.5% left of the starting time (0.5 h after hydration). At this moment, the content of physically bound water in cement pastes is few and hydration reaction is generally stable. And the time of entering steady period (>t_3) of 0.30NS0.0, 0.30NS1.0, 0.30NS1.5, 0.30NS2.0, and 0.30NS3.0 is 43.85, 42.22, 41.42, 40.60, and 39.75 h, respectively. This claims that the larger the NS dosage in cement paste, the earlier the steady period.

3.3. Effects of SAP on the NS Cement Paste Hydration. Figure 6 shows the influence of SAP on the TSA of NS cement pastes. It can be found that the TSA increases by the addition of SAP and increase with the SAP content increasing. This is because the internal curing water in SAP releases due to the difference in concentration and self-desiccation, which increase the amount of physically bound water.

In the initial period (0.0–t_1), the overall trend is consistent and the decline is small for different SAP contents according to Figure 6. TSA of 0.30NS1.5, 0.30NS1.5P0.15, and 0.30NS1.5P0.30 decreases 23.0, 42.0, and 67.0 a.u./g, respectively. Besides, compared with 0.30NS1.5, the initial period of 0.15% and 0.30% SAP contents of the samples extends to 0.27 and 0.44 h, respectively. It indicates that the

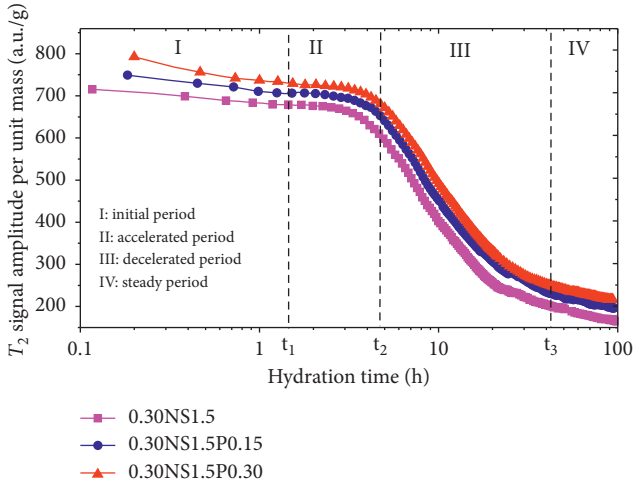

Figure 6: Effects of different SAP contents on the hydration process.

addition of SAP makes the initial period longer. That is because that when cement contacts with water, the concentration of Ca^{2+} in the paste increases rapidly. At this point, the water in SAP is seeping into the pore solution because of osmotic pressure, while the water reserved in SAP releases little at the beginning of the reaction. Therefore, the higher the content of SAP is, the more the water releases. Hence, the Ca^{2+} reaching saturation rate gets faster, which can extend the duration of the initial period. And this phenomenon is also consistent with the observation from Justs et al. [31].

When the hydration time is between t_1 and t_2, the slope of the curve becomes larger, which demonstrates that the hydration speed is accelerated. According to Table 6, the starting time of accelerated period of 0.30NS1.5, 0.30NS1.5 P0.15, and 0.30NS1.5 P0.30 is 1.45 h, 1.72 h, and 1.89 h, respectively, which means that the addition of SAP delays the arrival time of the accelerated period. At this period, owing to rapid hydration reaction, Ca^{2+} concentration increases constantly; therefore, the SAP releases water constantly due to the concentration difference in the paste. And the water release is positively correlated with the dosage of SAP. In addition, the accelerated period of 0.30NS1.5, 0.30NS1.5P0.15, and 0.30NS1.5P0.30 is 3.33, 4.2, and 4.49 h, respectively; this result shows that, with the increase of SAP, the accelerated period lasts longer.

In the decelerated period (t_2–t_3), the hydration rate of the paste gradually becomes slower, the hydration products meet, and the paste begins to harden. At the end of the decelerated period, TSA of 0.30S1.5, 0.30NS1.5P0.15, and 0.30NS1.5P0.30 is 202.1, 223.6, and 239.3 a.u./g, respectively. And the period of 0.30NS1.5, 0.30NS1.5 P0.15, and 0.30NS1.5 P0.30 lasts for 36.64, 42.67, and 45.07 h, respectively. It is because that the rising rate of Ca^{2+} concentration becomes slow in the decelerated period; therefore, the amount of water release of SAP also becomes slow.

With the increase of time, the paste enters a steady period ($>t_3$). There is a certain strength for the paste at this time. Besides, hydration products and the rest of the cement are also wrapped in the formed skeleton. SAP will still release moisture because of the desiccation of paste, but the rate of water release slows down. At 96 h, TSA of the 0.30NS1.5, 0.30NS1.5P0.15, and 0.30NS1.5P0.30 is only 165.5, 196.6, and 216.6 a.u./g, respectively, indicating that the physically bound water amount in the cement paste increases with the SAP content. Compared with 0.30NS1.5, the arrival of a steady period of the 0.30NS1.5P0.15 and 0.30NS1.5P0.30 is delayed for 7.25 and 10.03 h, respectively. It shows that the incorporation of SAP delays the arrival of a steady period. And the mechanism is also related to the added water introduced by SAP.

Table 6: The hydration separation period time of different SAP content cement pastes (h).

Sample	t_1	t_2	t_3
0.30NS1.5	1.45	4.78	41.42
0.30NS1.5P0.15	1.72	5.92	48.67
0.3SNS1.5P0.30	1.89	6.38	51.45

3.4. Hydration Model

3.4.1. Hydration Model of Pure Cement Pastes. A prediction model is needed to be established for predicting the cement paste hydration. A classic hydration model put forward by the Avrami–Erofeev equation [32] is in the form of the overall kinetic equation which is in a simplified expression and fewer parameters compared with other hydration models. The Avrami–Erofeev equation is expressed as follows:

$$\alpha(t) = 1 - \exp\left[-(kt)^n\right], \tag{1}$$

where $\alpha(t)$ represents the hydration degree, k and n are empirical parameters, and t is the age of cement paste, days.

Based on the Avrami–Erofeev equation, a modified model of the TSA in unit mass pure cement paste is described as follows:

$$T(t) = a - b\exp(-ct), \tag{2}$$

where $T(t)$ is the TSA in unit mass pure cement paste at t days and a, b, and c are the parameters gained by fitting on experimental results.

Parameters a, b, and c and the corresponding correlation are presented in Table 7.

The functions of parameters a, b, and c are gained by fitting the values of a, b, and c and are described as follows:

$$a = -15242\left(\frac{w}{c}\right)^2 + 12109.30\frac{w}{c} - 2130.63, \tag{3}$$

$$b = -29026\left(\frac{w}{c}\right)^2 - 22261.30\frac{w}{c} + 3652.28, \tag{4}$$

$$c = -0.20\left(\frac{w}{c}\right)^2 - 0.17\frac{w}{c} + 0.17. \tag{5}$$

Figure 7 shows the test data and fitted results of pure cement pastes with different w/c. The fitted results of the

Table 7: Fitting parameters and correlation of pure cement pastes with different w/c.

w/c	a	b	c	Correlation	Standard error
0.30	130.38	−413.77	0.099	0.995	0.040
0.35	240.48	−583.49	0.084	0.997	0.031
0.40	274.37	−608.08	0.068	0.998	0.020

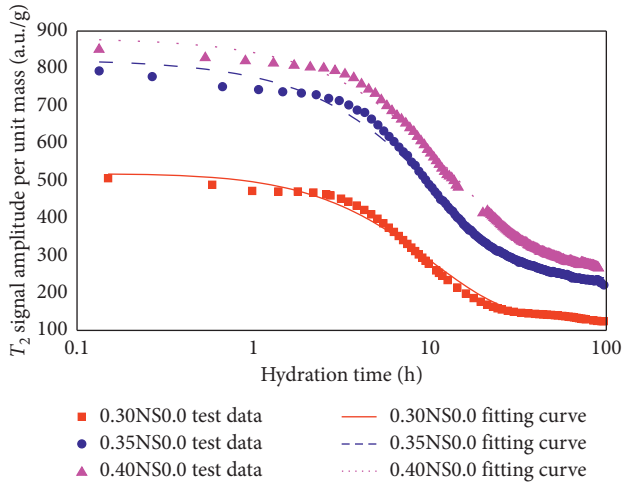

Figure 7: Experiment data and fitting results of pure cement pastes with different w/c.

prediction model are consistent with the experimental data. Therefore, the prediction model could well predict the TSA in a unit mass of pure cement paste. However, the fitted curves show some difference with the test data at the beginning of testing, while the fitting curves fit the test data well later.

3.4.2. Hydration Model of Cement Paste with the Addition of NS and SAP. The hydration model of cement paste with the addition of NS and SAP is proposed as in equation (6) based on the hydration model of pure cement paste:

$$T(t) = \gamma_{NS}\gamma_{SAP}[a - b\exp(-ct)], \quad (6)$$

where γ_{NS} and γ_{SAP} are the parameters relating to the NS and SAP contents. The equations of γ_{NS} and γ_{SAP} are the function of the NS or SAP dosage and age and fitted as follows:

$$\gamma_{NS} = d + e \times t^{0.1} + f \times t^{0.2}, \quad (7)$$

$$\gamma_{SAP} = m + n \times t + p \times t^{0.75}, \quad (8)$$

where d, e, and f are parameters related to the content of NS and m, n, and p are parameters related to the content of SAP.

Parameters d, e, and f and the corresponding correlation are presented in Table 8.

The functions of d, e, and f are obtained by fitting the values of parameters d, e, and f and are described as in equations (9)–(11):

Table 8: Fitting parameters and correlation of cement pastes with different NS dosages.

NS(%)	d	e	f	Correlation	Standard error
1.0	0.683	1.061	−0.483	0.995	0.041
1.5	−0.471	3.241	−1.353	0.993	0.047
2.0	0.183	2.349	−0.949	0.997	0.030
3.0	−2.712	7.406	−2.940	0.994	0.043

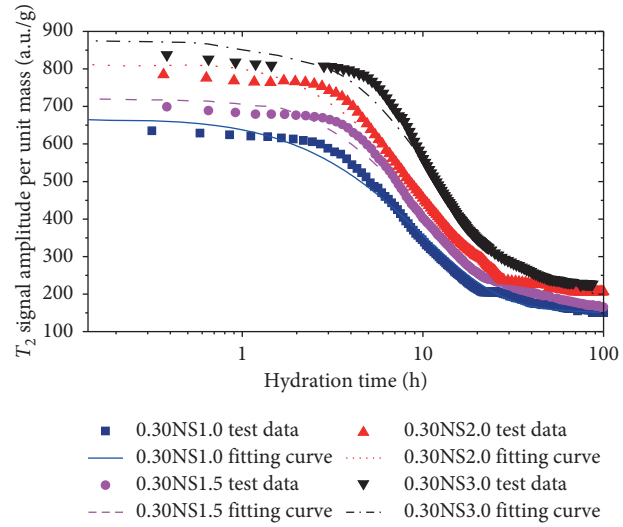

Figure 8: Experiment data and fitting results of NS cement pastes.

Table 9: Fitting parameters and correlation of cement pastes with different SAP dosages.

Sample	m	n	p	Correlation	Standard error
0.30NS1.5	1.010	0.002	−0.006	0.996	0.035
0.30NS1.5P0.15	1.024	−0.007	0.029	0.997	0.031
0.30NS1.5P0.30	1.037	−0.014	0.053	0.998	0.028

$$d = 0.683 \times m_{NS}^2 - 0.471 \times m_{NS} + 0.183 \times \ln(m_{NS}) - 2.712, \quad (9)$$

$$e = 14.475 \times m_{NS}^2 - 102.810 \times m_{NS} + 87.530 \times \ln(m_{NS}) + 89.392, \quad (10)$$

$$f = -5.954 \times m_{NS}^2 + 42.412 \times m_{NS} - 36.092 \times \ln(m_{NS}) - 36.942. \quad (11)$$

Figure 8 shows the test data and the fitted results of NS cement pastes. The evolution of the hydration model is consistent with the experimental data, so the modified model could well predict the TSA in a unit mass of NS cement pastes. However, the fitting curves also show some difference with the test data at the beginning of testing, while the fitting curves fit the test data well later.

Parameters m, n, and p are gained by fitting the test data of cement pastes containing NS and SAP and are shown in Table 9.

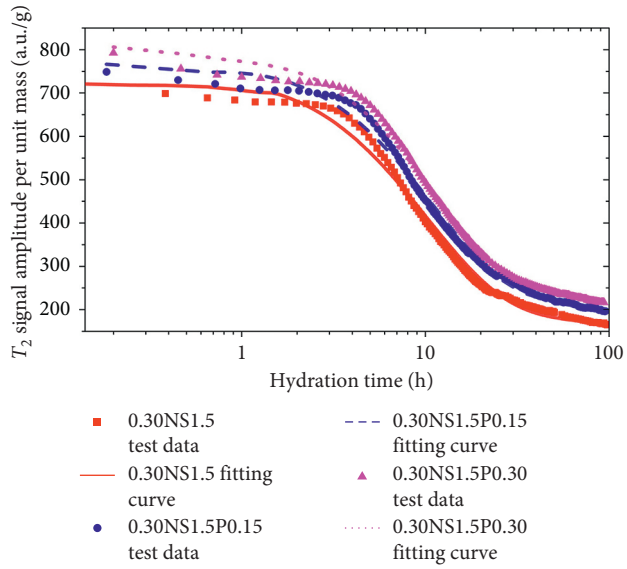

Figure 9: Experiment data and fitting results of cement pastes containing NS and SAP.

The functions of m, n, and p are gained by fitting the values of parameters m, n, and p and are described as in equations (12)–(14):

$$m = -0.022 \times m_{SAP}^2 + 0.097 \times m_{SAP} + 1.010, \quad (12)$$

$$n = 0.044 \times m_{SAP}^2 - 0.067 \times m_{SAP} + 0.002, \quad (13)$$

$$p = -0.244 \times m_{SAP}^2 + 0.270 \times m_{SAP} - 0.006. \quad (14)$$

Figure 9 shows the test results and the fitting results of cement pastes containing NS and SAP. The evolution of the hydration model is consistent with the experimental data. So the modified model could well predict the TSA in a unit mass of cement pastes containing NS and SAP. However, the fitting curves also show some difference with the test data at the beginning of testing, while the fitting curves fit the test data well later.

4. Conclusions

(i) The TSA in the unit mass of all cement pastes samples decreases with the hydration time. The cement paste hydration shows a four-stage pattern, i.e., the initial, accelerated, decelerated, and steady periods.

(ii) The TSA in the unit mass cement paste increases with w/c. The beginning time and the duration of each period are prolonged with increasing w/c.

(iii) The TSA in the unit mass cement paste increases with the NS content. The beginning time and the duration of each period are shortened with the increasing NS content, which became noticeable with the increase of the content of NS.

(iv) The TSA in the unit mass NS cement paste increases by the SAP addition and increases with the SAP content. The beginning time and the duration of each period are prolonged with the increasing SAP content.

(v) Based on the model put forward by Avrami–Erofeev, a modified hydration model taking the influences of NS and SAP into account is proposed, and the fitted results are consistent with the test results.

Data Availability

The test data used to support the findings of this study are included within the supplementary information file. The test data are included within the article and can be made freely available.

Conflicts of Interest

The authors declare that they have no conflicts of interest.

Acknowledgments

This research was funded by the National Natural Science Foundation of China under Grant no. 51708265, Jiangsu Planned Projects for Postdoctoral Research Funds under Grant no. 1501013C, the Natural Science Foundation of the Higher Education Institutions of Jiangsu Province under Grant no.16KJB560004, the Natural Science Foundation of Jiangsu Province of China under Grant no.BK20160106, the Research Foundation for Talented Scholars of Jinling Institute of Technology under Grant no.1636, Fund for Postgraduate Research and Practice Innovation Program of Jiangsu Province (SJCX18_0186), and the Fundamental Research Fund for the Central Universities (2018B760X14).

References

[1] S. Wei, D. Yi, C. Miao et al., "Application of organic-and nanoparticle-modified foams in foamed concrete: reinforcement and stabilization mechanisms," *Cement & Concrete Research*, vol. 106, pp. 12–22, 2018.

[2] Y. Ling, P. Zhang, J. Wang et al., "Effect of PVA fiber on mechanical properties of cementitious composite with and without nano-SiO_2," *Construction and Building Materials*, vol. 229, 2019.

[3] M. Oltulu and R. Şahin, "Effect of nano-SiO_2, nano-Al_2O_3 and nano-Fe_2O_3 powders on compressive strengths and capillary water absorption of cement mortar containing fly ash: a comparative study," *Energy and Buildings*, vol. 58, no. 2, pp. 292–301, 2013.

[4] D. Wang, Q. Wang, and Z. Huang, "Investigation on the poor fluidity of electrically conductive cement-graphite paste: experiment and simulation," *Materials & Design*, vol. 169, Article ID 107679, 2019.

[5] H. Zhao, K. Jiang, R. Yang, Y. Tang, and J. Liu, "Experimental and theoretical analysis on coupled effect of hydration, temperature and humidity in early-age cement-based materials," *International Journal of Heat and Mass Transfer*, vol. 146, Article ID 118784, 2020.

[6] H. Zhao, X. Wu, Y. Huang, P. Zhang, Q. Tian, and J. Liu, "Investigation of moisture transport in cement-based

materials using low-field nuclear magnetic resonance imaging," *Magazine of Concrete Research*, pp. 1–19, 2019.

[7] P. Zhang, S. Fu, K. Zhang, and T. Zhang, "Mechanical properties of polyvinyl alcohol fiber-reinforced concrete composite containing fly ash and nano-SiO_2," *Science of Advanced Materials*, vol. 10, no. 6, pp. 769–778, 2018.

[8] Q. Ye, "Comparison of volcanic activity of Nano-SiO_2 and silica powders," *Concrete*, vol. 137, no. 3, pp. 19–22, 2001, in Chinese.

[9] Y. Qing, Z. Zenan, S. Li, and C. Rongshen, "A comparative study on the pozzolanic activity between nano-SiO2 and silica fume," *Journal of Wuhan University of Technology-Materials Science Edition*, vol. 21, no. 3, pp. 153–157, 2006.

[10] Y. Qing, Z. Zenan, K. Deyu, and C. Rongshen, "Influence of nano-SiO_2 addition on properties of hardened cement paste as compared with silica fume," *Construction and Building Materials*, vol. 21, no. 3, pp. 539–545, 2007.

[11] M.-H. Zhang, J. Islam, and S. Peethamparan, "Use of nano-silica to increase early strength and reduce setting time of concretes with high volumes of slag," *Cement and Concrete Composites*, vol. 34, no. 5, pp. 650–662, 2012.

[12] A. M. Said, M. S. Zeidan, M. T. Bassuoni, and Y. Tian, "Properties of concrete incorporating nano-silica," *Construction and Building Materials*, vol. 36, no. 4, pp. 838–844, 2012.

[13] N. B. Singh, M. Kalra, and S. K. Saxena, "Nanoscience of cement and concrete," *Materials Today: Proceedings*, vol. 4, no. 4, pp. 5478–5487, 2017.

[14] L. Senff, D. Hotza, S. Lucas, V. M. Ferreira, and J. A. Labrincha, "Effect of nano-SiO_2 and nano-TiO_2 addition on the rheological behavior and the hardened properties of cement mortars," *Materials Science and Engineering: A*, vol. 532, pp. 354–361, 2012.

[15] B. Guo, R. Sun, and F. Zheng, "Experimental study of concrete autogenous shrinkage with superfine active silica," *Beton Chinese Edition-Ready-Mixed Concrete*, no. 1, pp. 24–28, 2007, in Chinese.

[16] L. P. Esteves, *Internal Curing in Cement-Based materials*, PhD Thesis, Aveiro University, Aveiro, Portugal, 2009.

[17] J. Justs, M. Wyrzykowski, D. Bajare, and P. Lura, "Internal curing by superabsorbent polymers in ultra-high performance concrete," *Cement and Concrete Research*, vol. 76, pp. 82–90, 2015.

[18] V. Tydlitát, T. Matas, and R. Č tas, "Effect of w/c and temperature on the early-stage hydration heat development in Portland-limestone cement," *Construction and Building Materials*, vol. 50, no. 2, pp. 140–147, 2014.

[19] L. Xiao and Z. Li, "Early-age hydration of fresh concrete monitored by non-contact electrical resistivity measurement," *Cement and Concrete Research*, vol. 38, no. 3, pp. 312–319, 2008.

[20] J. P. Gorce, N. B. Milestone, and P. J. Mcdonald, "Probing the water phases and microstructure in a model cement blend matrix used for the encapsulation of intermediate level nuclear wastes," *MRS Online Proceeding Library*, vol. 932, 2005.

[21] A. Plassais, M. P. Pomiès, N. Lequeux et al., "Microstructure evolution of hydrated cement pastes," *Physical Review E Statistical Nonlinear & Soft Matter Physics*, vol. 72, no. 4, 2005.

[22] T. Apih, G. Lahajnar, A. Sepe et al., "Proton spin-lattice relaxation study of the hydration of self-stressed expansive cement," *Cement and Concrete Research*, vol. 31, no. 2, pp. 263–269, 2001.

[23] A. She, W. Yao, and Y. Wei, "In-situ monitoring of hydration kinetics of cement pastes by low-field NMR," *Journal of Wuhan University of Technology-Materials Science Edition*, vol. 25, no. 4, pp. 692–695, 2010.

[24] S. An-ming and Y. Wu, "Research on hydration of cement at early age by proton NMR," *Journal of Building Materials*, vol. 13, no. 3, pp. 376–379, 2010, in Chinese.

[25] H. Zhao, G. Sun, L. Yu et al., "Hydration of early age cement paste with nano-caco3 and sap by lf-nmr spectroscopy: mechanism and prediction," *Modelling and Simulation in Engineering*, vol. 2019, Article ID 8384051, 10 pages, 2019.

[26] ASTM, *Standard Practice for Mechanical Mixing of Hydraulic Cement Pastes and Mortars of Plastic Consistency*, ASTM, West Conshohocken, PA, USA, 1999.

[27] R. Berliner, M. Popovici, K. W. Herwig, M. Berliner, H. M. Jennings, and J. J. Thomas, "Quasielastic neutron scattering study of the effect of water-to-cement ratio on the hydration kinetics of tricalcium silicate," *Cement and Concrete Research*, vol. 28, no. 2, pp. 231–243, 1998.

[28] P. Kumar Mehta and P. J. M. Monteiro, *Concrete Miscrostructure, Properities and Materials*, University of California-Berkeley, Berkeley, CA, USA, 2006.

[29] B. A. Hengjing, Q. Feng, and Y. Yang, "Hydration reaction between C3S and fly ash, silica fume, nano-SiO_2 and microstructure of hydrated pastes," *Journal of the Chinese Creamic Society*, vol. 30, no. 6, pp. 780–784, 2002, in Chinese.

[30] G. Land and D. Stephan, "The influence of nano-silica on the hydration of ordinary Portland cement," *Journal of Materials Science*, vol. 47, no. 2, pp. 1011–1017, 2012.

[31] J. Justs, M. Wyrzykowski, F. Winnefeld, D. Bajare, and P. Lura, "Influence of superabsorbent polymers on hydration of cement pastes with low water-to-binder ratio," *Journal of Thermal Analysis and Calorimetry*, vol. 115, no. 1, pp. 425–432, 2014.

[32] K. van Breugel, "Simulation of Hydration and Formation of Structure in Hardening Cement-Based materials," PhD Thesis, Delft University of Technology, Delft, Netherlands, 1991.